Acta Crystallographica Section B
Structural Science
ISSN 0108-7681

Experimental electron density of urea–phosphoric acid (1/1) at 100 K

Bernardo Lages Rodrigues,[a] Roland Tellgren[b] and Nelson G. Fernandes[a]*

[a]Department of Chemistry, Federal University of Minas Gerais, CP702, 31270-901 Belo Horizonte, Brazil, and [b]Department of Inorganic Chemistry, The Angstrom Laboratory, Uppsala University, Box 538, SE-751 21, Sweden

Correspondence e-mail: nelsongf@cenapad.ufmg.br

Received 5 July 2000
Accepted 12 March 2001

The deformation electron density of the urea–phosphoric acid adduct has been studied from 100 K X-ray and neutron diffraction experiments. Data were interpreted according to the Hirshfeld model. The long hydrogen bonds show characteristics of electrostatic interaction. Deformation density maps on the short hydrogen bond shows hydrogen more strongly bonded to urea than to phosphoric acid, and peak maxima at almost midway between the two O—H bonds.

1. Introduction

Urea was the subject of two very accurate experimental electron density studies. One of these (Swaminathan, Craven & McMullan, 1984) was performed at 123 K and illustrated the efficiency of deformation models to describe this non-centrosymmetric system. The other study (Zavodnik *et al.*, 1999) was performed with data collected at 148 K and discussed the importance of correcting data for thermal diffuse scattering. The electron density of phosphoric acid has also been the subject of a very accurate experimental study (Souhassou *et al.*, 1995), which shows the influence of hydrogen bonding on the polarization of P—O bonds. These multipole studies agree well with *ab initio* calculations for crystalline urea (Dovesi *et al.*, 1990) and phosphoric acid (Moss *et al.*, 1995). The crystal structures of urea (Swaminathan, Craven, Spackman & Stewart, 1984) and phosphoric acid (Blessing, 1988) were also determined by neutron diffraction.

Reaction between urea and phosphoric acid gives a solid adduct. Previous works based on room-temperature X-ray (Motz & Albrand, 1972) and neutron (Konstansek & Busing, 1972) data show that the crystalline adduct is stabilized by many hydrogen bonds, including a short intramolecular O—H···O bond [d(O···O) = 2.421 Å from neutron data]. Previous X-ray and neutron (X-N) studies of the adduct (Savage *et al.*, 1987) suggest that the short hydrogen bond should be interpreted as a three-centre, four-electron bond. Therefore, an accurate study on the electron density of urea–phosphoric acid [$H_3PO_4{\cdot}CO(NH_2)_2$] can contribute to the understanding of the nature of short hydrogen bonds. We present here an experimental electron density study of $H_3PO_4{\cdot}CO(NH_2)_2$ by neutron and high-resolution X-ray ($\sin\theta/\lambda \leq 1.19$ Å^{-1}) diffraction methods. Data were collected at 100 K, since thermal vibrational effects are less correlated to electron density parameters at low temperatures (Hirshfeld, 1976).

Table 1
Experimental details.

	Neutron	X-ray
Crystal data		
Chemical formula	$CH_7N_2O_5P$	$CH_7N_2O_5P$
Chemical formula weight	159	159
Cell setting, space group	Orthorhombic, *Pbca*	Orthorhombic, *Pbca*
a, *b*, *c* (Å)	17.43 (2), 7.43 (2), 8.97 (2)	17.4527 (7), 7.4465 (5), 8.9589 (4)
V (Å^3)	1161 (4)	1164.31 (9)
Z	8	8
D_x (Mg m^{-3})	1.820	1.815
Radiation type	Neutron	Mo $K\alpha$
Wavelength (Å)	1.207	0.71073
No. of reflections for cell parameters	9	98
θ range (°)	18.9–30.9	12–20
μ (mm^{-1})	2.225 (obs.)	0.431 (calc.)
Temperature (K)	100	100
Crystal form, colour	Prismatic, colourless	Almost spherical, colourless
Crystal size (mm)	3.8 × 2.2 × 1.0	–
Crystal radius (mm)	–	0.19
Data collection		
Diffractometer	Huber four-circle	Siemens P4
Data collection method	θ–2θ scans	θ–2θ scans
Absorption correction	Analytical	Analytical
T_{min}	0.55	0.87
T_{max}	0.66	0.89
No. of measured, independent and observed parameters	1762, 1599, 1579	8472, 7433, 7257
Criterion for observed reflections	$I > -3\sigma(I)$	$I > 0.0\sigma(I)$
R_{int}	0.017	0.0134
θ_{max} (°)	52	60
Range of *h*, *k*, *l*	$-22 \rightarrow h \rightarrow 0$ $-9 \rightarrow k \rightarrow 0$ $0 \rightarrow l \rightarrow 11$	$-1 \rightarrow h \rightarrow 41$ $-1 \rightarrow k \rightarrow 17$ $-1 \rightarrow l \rightarrow 21$
Intensity decay (%)	0	1.1
Refinement		
Refinement on	F^2	F^2
$R[F^2 > 2\sigma(F^2)]$, $wR(F^2)$, *S*	0.053, 0.053, 1.35	0.0577, 0.053, 0.69
No. of reflections and parameters used in refinement	1579, 151	7257, 215
H-atom treatment	Refined anisotropically	Hydrogen fixed from neutron
Weighting scheme	$w = 1/[\sigma^2(F_o^2)]$	$w = 1/[\sigma^2(F_o^2) + 0.0068F_o^2 + 34.9\lambda/\sin\theta - 0.00055F_o^2\lambda/\sin(\theta)]$
$(\Delta/\sigma)_{max}$	0.001	0.001
$\Delta\rho_{max}$, $\Delta\rho_{min}$ (nuclei Å)	0.38, −0.19	0.61, −0.62
Extinction method	See text	See text

Computer programs used: *XSCANS* (Siemens, 1991), *P4red*, *DUPALS* (Lundgren, 1982), *ORTEP*3 (Burnet & Johnson, 1996), *FOPLOT* (Lundgren, 1982), *ARACOR* (Lundgren, 1982), Ms-DOS 6.0 editor.

2. Experimental

2.1. Crystal growth

Solid $H_3PO_4{\cdot}CO(NH_2)_2$ is obtained from an equimolar aqueous solution of urea and phosphoric acid. Recrystallization in methanol gives single crystals suitable for X-ray diffraction experiments. One of these was chosen and measured on a Siemens P4 diffractometer equipped with a nitrogen cryosystem. Another was selected as a seed to grow the single crystal used in the neutron data collection procedure. The sample was obtained by slow evaporation of a saturated methanolic solution.

2.2. Data collection

Neutron diffraction data were collected at the Swedish Research Reactor, R2, in Studsvik, with a flux at the crystal location of approximately 1.15×10^4 neutron mm^{-2} s^{-1}. Experimental details are given in Table 1.[1] Lorentz and absorption corrections were applied using the program package of the Institute of Chemistry, Uppsala University (Lundgren, 1982).

X-ray data were collected on a Siemens P4 diffractometer equipped with a low-temperature device. Data collection features are given in Table 1. Data were corrected by Lorentz, polarization and absorption effects. This latter correction was performed analytically by Gaussian numerical quadrature over a 6 × 6 × 6 grid.

3. Refinements

3.1. Neutron data

Neutron scattering lengths given in *International Tables for Crystallography* (Sears, 1995) were used. Starting from room-temperature neutron diffraction results (Konstansek & Busing, 1972), the positional and isotropic thermal displacement parameters of non-H atoms were refined using the 1579 observed reflections. Then, H atoms were located in the Fourier-difference synthesis and anisotropic displacement parameters for all atoms were introduced. This refinement resulted in non-positive displacement parameters for P and C atoms. Isotropic and anisotropic extinction models of Becker & Coppens (1974, 1975) were applied to solve this problem. The best results were obtained with anisotropic type I extinction and Lorentzian distribution of mosaic blocks. Therefore, in the final neutron refinement 144 atomic and 6 anisotropic extinction parameters, as well as the scale factor, were refined, resulting in 151 refined parameters. The drawing of the molecule is shown in Fig. 1 and the main results of the refinement are given in Table 1.

3.2. X-ray data

3.2.1. Conventional refinements and extinction correction. The refinements started from positional and displacement parameters obtained from neutron diffraction data. X-ray scattering factors given by Maslen *et al.* (1995) were used. First

[1] Supplementary data for this paper are available from the IUCr electronic archives (Reference: CA0006). Services for accessing these data are described at the back of the journal.

of all isotropic extinction models of Becker and Coppens were tested. During the extinction tests, positional and anisotropic thermal displacement parameters of non-H atoms were refined, as well as the scale factor and the extinction parameter. All extinction correction models gave negative extinction parameters and did not improve the statistical errors. Therefore, extinction corrections for X-ray diffraction data were not considered.

3.2.2. Multipole refinements. Positional and displacement parameters obtained from neutron diffraction data are used as a starting point for multipole refinements. These refinements consider the asphericity of electron distribution as an expansion of functions according to the method proposed by Hirshfeld (1971) and modified by Harel & Hirshfeld (1975), and Hirshfeld (1977). The model expresses the non-sphericity of electron distribution by an expansion of up to 35 terms centred on each atom. In this way, the expansion functions have the following general form on each atomic centre

$$\delta\rho_a = \sum_l c_{a,l}\rho_{a,l}, \text{ with}$$

$$\rho_{a,l}(\mathbf{r}) = \rho_n(r_a, \theta_k) = N_n r^n e^{-\gamma r^m} \cos^n \theta_k,$$

where r and θ are polar coordinates in the kth of a chosen set of axes; n and k are integers [n = 0–4; k = 1 to $(n + 1)(n + 2)/2$]; m is 1 or 2, indicating exponential or Gaussian dependence of the radial part of the expansion functions $\delta\rho_a$; N_n is a normalization factor and l is a summation of k terms up to n = 4. The method refines parameters $c_{a,l}$.

Functions with $n \leq 4$ for non-H atoms and H4 were used in the least-squares refinement. Functions with $n \leq 3$ were used for all other H atoms. The best results were obtained assuming Gaussian dependence of radial functions (m = 2). Local symmetries have been adopted in order to reduce the number of refined parameters. In this way, the multipole refinement started with the following local symmetry on each atom: *mm*2 for P, O2, O4, O5, N1, N2 and C; *m* for O1 and O3; cylindrical for all hydrogens except H4, for which an inversion centre was added to cylindrical symmetry. O1 and O3 were assumed to be chemically equivalent, as well as N1 and N2. H atoms bonded to chemically equivalent atoms were also assumed to be chemically equivalent. Following the purpose of obtaining a better description of the chemical bonds, atomic symmetries were systematically lowered. Statistical parameters R and wR, as well as deformation maps, served as a guide to choose the best refinement. Different atomic local symmetries were tested: *mm*2, 2 and 1 for P, O2, O4 and O5; *m* and 1 for O1 and O3; *mm*2 and *m* for N atoms; cylindrical, with and without an inversion centre, for hydrogen H4, involved in the short hydrogen bond. The radial exponential factors γ could not be refined along with other parameters.

In the final refinement, the chemical equivalences between different atoms were kept as those of the starting multipole refinement. The local symmetries assumed were *mm*2 for P, O2, O4, C and N1; *m* for O1 and O5; cylindrical plus an inversion centre for H4; cylindrical for all other H atoms. The radial exponential factors were set to 2.5 for P; 3.5 for O1; 4.5 for O2, O4 and O5; 5.0 for N; 2.5 for H1; 2.2 for H11 and 2.0 for H4. In the last cycle one scale factor, 27 positional parameters, 54 anisotropic displacement parameters and 133 coefficients of multipole functions were refined. The positional and anisotropic displacement parameters for the H atoms were fixed at their refined neutron values. The main results of this refinement, for which deformation maps are discussed, are shown in Table 1, for which deformation maps are also discussed in the next section. Atomic positions and equivalent isotropic. displacement parameters have been deposited.

Table 2
Bond distances (Å) and angles (°).

P—O1	1.562 (2)	O1—H1	1.000 (3)
P—O2	1.512 (2)	O3—H3	1.005 (3)
P—O3	1.554 (2)	N1—H11	1.016 (3)
P—O4	1.517 (2)	N1—H12	1.004 (3)
C—N1	1.323 (1)	N1—H12	1.017 (3)
C—N2	1.325 (1)	N2—H22	1.003 (3)
C—O5	1.295 (2)		
O1—P—O2	111.4 (1)	P—O1—H1	113.5 (2)
O1—P—O3	108.3 (1)	P—O3—H3	117.0 (2)
O1—P—O4	105.5 (1)	P—O4—H4	125.1 (2)
O2—P—O3	106.6 (1)	C—N1—H11	118.6 (2)
O2—P—O4	113.6 (1)	C—N1—H12	120.2 (2)
O3—P—O4	111.3 (1)	H11—N1—H12	120.8 (2)
O5—C—N1	118.3 (1)	C—N2—H21	120.4 (2)
O5—C—N2	121.0 (1)	C—N2—H22	120.5 (2)
N1—C—N2	120.8 (1)	H21—N2—H22	119.0 (2)

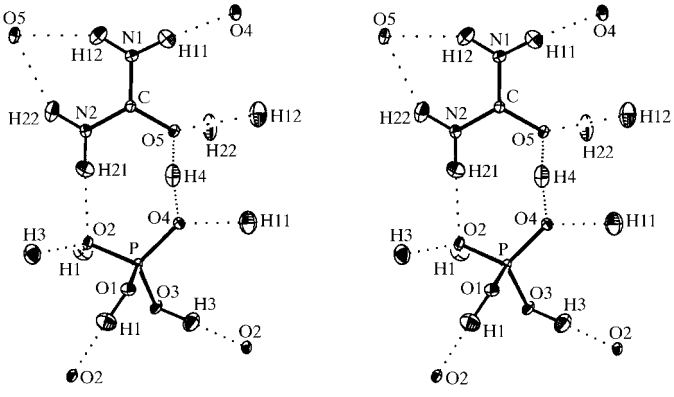

Figure 1
*ORTEP*3 (Burnet & Johnson, 1996) stereoscopic view of the molecule and its hydrogen-bonded neighbours. The ellipsoids correspond to 50% probability.

4. Results and discussion

4.1. Geometrical features

Phosphorous is tetrahedally coordinated and the urea region is almost planar, as can be seen in Fig. 1. Bonds between phosphorous and hydroxyl O atoms are longer than P—O2 and P—O4 (Table 2). These features are the same as those observed by Konstansek & Busing (1972).

Table 3
Hydrogen-bond parameters (Å, °).

A—H···B	A···B (Å)	A—H (Å)	H—B (Å)	A—H···B (°)
O1—H1···O2^{i}	2.649 (2)	1.000 (1)	1.643 (3)	174.4 (3)
O3—H3···O2^{ii}	2.589 (2)	1.005 (1)	1.584 (3)	177.4 (3)
O4—H4···O5	2.410 (2)	1.259 (1)	1.160 (3)	170.2 (3)
N1—H11···O4^{iii}	2.893 (2)	1.016 (1)	1.885 (3)	171.4 (2)
N1—H12···O5^{iv}	3.090 (2)	1.004 (1)	2.221 (3)	143.9 (2)
N2—H21···O2	2.943 (2)	1.017 (1)	1.936 (3)	170.1 (2)
N2—H22···O5^{iv}	3.064 (2)	1.003 (1)	2.180 (3)	146.2 (2)

Symmetry codes: (i) $\frac{1}{2}-x,-\frac{1}{2}+y,z$; (ii) $x,\frac{1}{2}-y,-\frac{1}{2}+z$; (iii) $1-x,\frac{1}{2}+y,\frac{1}{2}-z$; (iv) $x,\frac{3}{2}-y,\frac{1}{2}+z$.

The room-temperature neutron diffraction study of $H_3PO_4{\cdot}CO(NH_2)_2$ shows H4 nearer O5 than O4, and Olovsson & Jönsson (1976) classified the short hydrogen bond of the adduct as non-centred. As can be seen in Table 3, the refinement of H4 positional parameters from the present 100 K neutron data shows a similar displacement from the centre of the bond. Thus, this indicates that H4 is more strongly bonded to O5 than to O4, in agreement with room-temperature refinement. Fig. 1 shows the network of hydrogen bonds in the crystal.

4.2. Hirshfeld rigid-bond test

Correlation between electron-density distribution and atomic displacement is a problem in electron density studies. Hirshfeld (1976) postulated, as a measure of confidence in the displacement parameters, that the relative vibration of any pair of covalently bonded atoms has an effectively null component in the bonding direction. This means that $|(UA)^2 - (UB)^2|$ shall vanish for a pair of covalently bonded atoms A and B, where $(UA)^2$ and $(UB)^2$ are the mean-square amplitudes of the vibration of atoms A and B along the A—B bond.

Table 4
Mean-square vibration amplitudes (Å^2 × 10^4) of bonded non-H atoms A and B for the rigid-bond test of vibration parameters of the final multipole refinement.

A	B	$(UA)^2$	$(UB)^2$	$\lvert(UA)^2-(UB)^2\rvert$
P	O1	97 (4)	100 (10)	3 (10)
P	O2	75 (6)	78 (11)	3 (13)
P	O3	77 (6)	77 (11)	0 (13)
P	O4	84 (4)	86 (11)	2 (12)
C	N1	94 (13)	95 (13)	1 (18)
C	N2	92 (13)	85 (13)	7 (18)
C	O5	97 (14)	89 (11)	8 (18)
Mean				3 (6)

As can be seen from Table 4, $|(UA)^2 - (UB)^2|$ is statistically equal to zero for all non-H A—B bonds of the adduct and, consequently, the Hirshfeld postulate is satisfied. Therefore, the conclusion is that the atomic displacements are well described in the multipole refinement, and that the refinement succeeded in distinguishing between non-spherical valence electron distribution and the atomic displacements.

4.3. Deformation electron densities

Static deformation electron density maps are shown in Figs. 2–5. Fig. 4(*b*) and Fig. 5(*f*) also include dynamic deformation density maps, which would allow a better judgement of the data quality. Anyhow, the overall features in bonding and non-bonding regions shown in these maps are, qualitatively, similar to those found in the previous X-N study of the urea–phosphoric acid adduct at room temperature (Savage *et al.*, 1987).

4.3.1. Phosphoric acid region. Deformation densities in O—P—O planes are shown in Fig. 2. The P—O2 bond has a maximum peak of 0.59 e Å^{-3}. On the other hand, P—O1(H) and P—O3(H) have peak maxima of 0.44 e Å^{-3} (O1 and O3 were assumed to be chemically equivalent). Therefore, the peak height is higher for the P—O bond than for P—O(H) bonds, as expected from the double bond–single bond character. It is very interesting to notice the intermediate value for

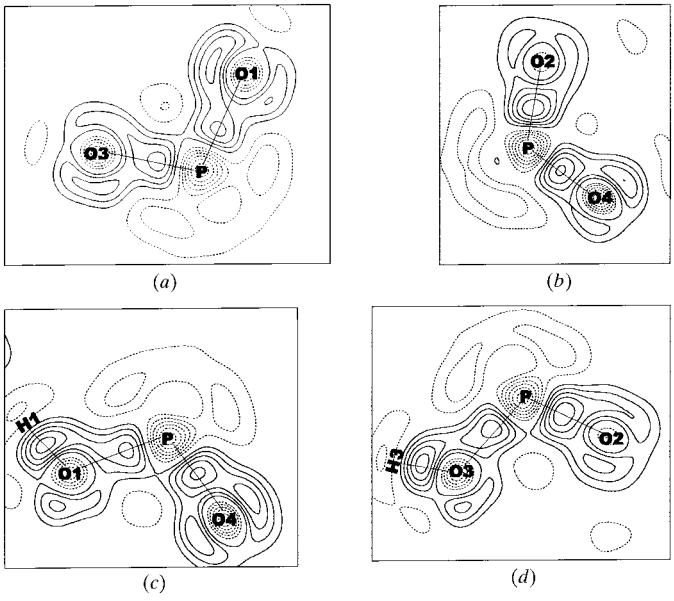

Figure 2
Static deformation density maps in the planes defined by atoms (*a*) P, O1 and O3; (*b*) P, O2 and O4; (*c*) P, O1 and O4; (*d*) P, O2 and O3. Contour interval 0.10 e Å^{-3}; negative contours dotted and positive contours solid.

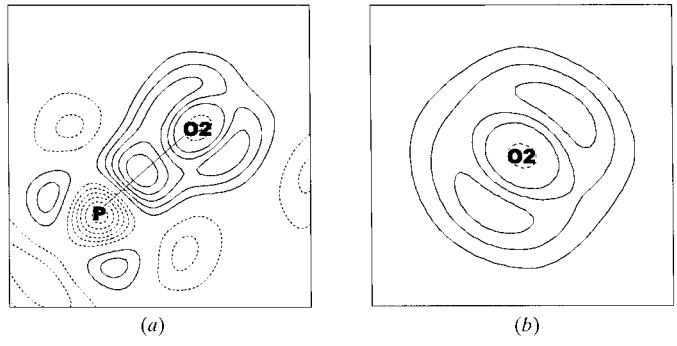

Figure 3
Static deformation density maps in the planes (*a*) perpendicular to the plane O2—P—O4 throughout the line of P—O2; (*b*) perpendicular to the P—O2 bond, 0.1 Å behind the oxygen O2. Contours levels defined as for Fig. 2.

the peak height of the P—O4 bond: 0.53 e Å^{-3}. This can be explained in terms of hydrogen bonding: the O4 atom is involved in the short hydrogen bond, with d(O4—H4) = 1.259 (1) Å. Therefore, it is expected, for the P—O4(H4) bond, a bond order which is higher than a single P—O(H) bond, but smaller than a double P═O bond. These results are clearly distinct from the previous results on a crystal of phosphoric acid (Souhassou *et al.*, 1995), where three approximately similar P—O(H) interactions and a double P═O bond are seen. In this way, it may be said that the adduct formation strengthens one P—O(H) interaction and decreases the strength of the P═O interaction of the phosphoric acid.

It is also worthwhile to comment on the electron density distribution around O2 and O4. In Fig. 2(*b*) the plane defined by P, O2 and O4 shows three electron density maxima around O4. In this plane the P—O4 bond, an intense lobe directed through the short hydrogen bond, and a weak lobe in the direction of a long intermolecular hydrogen bond can be seen.

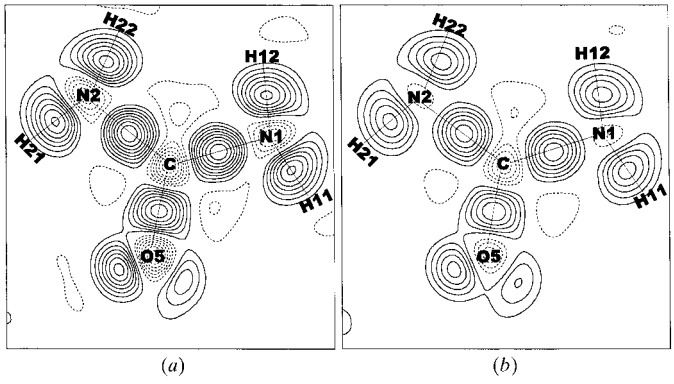

Figure 4
(*a*) Static and (*b*) dynamic deformation density maps in the mean plane defined by atoms C, O5, N1 and N2. Contours levels defined as for Fig. 2.

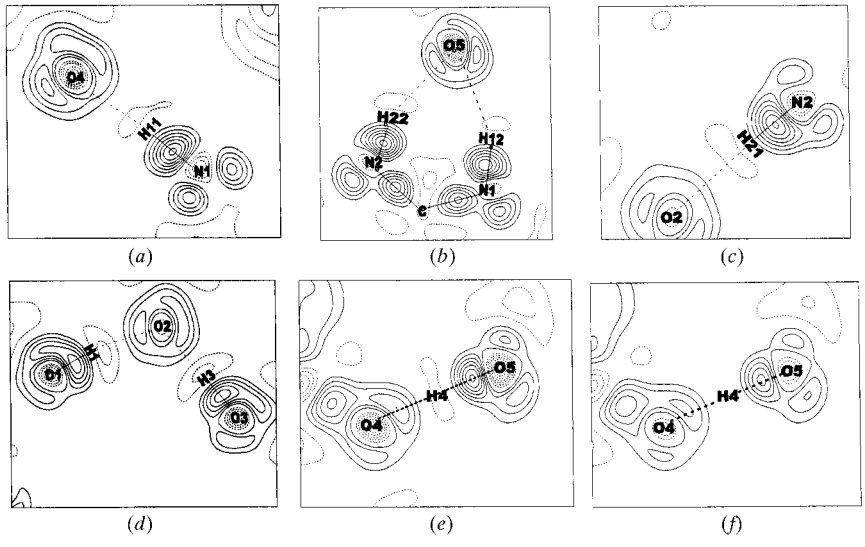

Figure 5
Static deformation density maps in the planes defined by: (*a*) N1—H11···O4; (*b*) H12···O5···H22; (*c*) N2—H21···O2; (*d*) H1···O2···H3; (*e*) O5···H4···O4; (*f*) dynamic deformation density map in the plane defined by O5···H4···O4. Contours levels defined as for Fig. 2.

However, as shown in Fig. 3, around O2 there are two electron density maxima which lie in a plane orthogonal to the plane defined by P, O2 and O4. Therefore, π-bond contribution between P—O2 and P—O4 appear to lie in perpendicular directions. These results are in agreement with those deduced theoretically by Cruickshank (1961).

4.3.2. Urea region. The deformation density map in the plane defined by the urea molecule (Fig. 4) presents two C—N bonds with peak maxima near 0.80 e Å^{-3}, the C—O5 bond with a peak maximum of 0.73 e Å^{-3}. These features are similar to those obtained in the previous deformation density study of urea crystals (Swaminathan, Craven & McMullan *et al.*, 1984). In urea, the two non-bonding regions are very similar, with the same peak height, probably due to the highest π-bond contribution. On the other hand, in this present study, in the O5—H4 direction (short hydrogen bond) the peak height is 0.71 e Å^{-3}, while the lone pair region is much more diffuse with a peak height of 0.35 e Å^{-3} in the urea plane, probably due to the O5 environment. Figs. 5(*b*) and (*e*) show that O5 is involved in three hydrogen bonds.

4.3.3. Hydrogen bonds. Deformation densities through long hydrogen bonds are shown in Figs. 5(*a*)–(*d*). Excess charge density is found for the O—H and N—H covalent bonds, as well as near O atoms in the direction of the long O···H bonds. There are regions of electron depletion on the weakly bonded side of the H atoms. These features are typical for hydrogen bonds of moderate strength [see *e.g.* Coppens (1997), ch. 12].

The static deformation density map of the plane defined by the short hydrogen bond is shown in Fig. 5(*e*). The dynamic deformation density is shown in Fig. 5(*f*). Electron depletion near atomic positions and deformation density peaks almost midway between the two O—H bonds, with a peak maximum of 0.71 e Å^{-3} between O5 and H4, and of 0.40 e Å^{-3} between O4 and H4. At this time, it is helpful to compare the map of the short hydrogen bond of urea–phosphoric acid (present work) with the maps of other compounds containing short symmetric hydrogen bonds, such as $NaH(CH_3COO)_2$ (Stevens *et al.*, 1977), $Na_5H_3(CO_3)_4$ (Fernandes *et al.*, 1990*a*), $KNiH(CO_3)_2{\cdot}4H_2O$ (Fernandes *et al.*, 1990*b*), $(NH_3CH_3)(C_4H_5O_4){\cdot}H_2O$ (Flensburg *et al.*, 1995) and (NH_3CH_3)-$(C_4H_3O_4)$ (Madsen *et al.*, 1998). All short hydrogen bonds present maps showing electron depletion near atomic positions and electron density peaks in bonding regions. This feature indicates some covalent character for the two O—H interactions of each hydrogen bond, as stated by Stevens *et al.* (1977) for $NaH(CH_3COO)_2$. In contrast, urea–phosphoric acid clearly shows two distinct O—H interactions: a stronger interaction between H4 and O5, with a peak height of 0.71 e Å^{-3}, and a weaker interaction between H4 and O4, with a peak height

of 0.40 e Å^{-3}. This difference is caused by the different chemical environments of O5 and O4. Refinements using the Hansen & Coppens (1978) formalism, as implemented in the *XD* program (Koritsanszky *et al.*, 1995), are also in this direction: there is one (3,−1) critical point for each O—H bond of the short hydrogen bond. The topological descriptors of the O4—H4 (3,−1) critical point (CP) are $\rho = 1.02$ e Å^{-3}, $\lambda_1 = -11.18$ e Å^{-5}, $\lambda_2 = -11.15$ e Å^{5}, $\lambda_3 = 11.75$ e Å^{5}, $\nabla^2\rho = -10.58$ e Å^{-5}, d(O4—CP) = 0.97 Å and d(H4—CP) = 0.30 Å. The descriptors of the O5—H4 (3,−1) CP are $\rho = 1.20$ e Å^{-3}, $\lambda_1 = -16.87$ e Å^{-5}, $\lambda_2 = -16.82$ e Å^{-5}, $\lambda_3 = 15.22$ e Å^{-5}, $\nabla^2\rho = -18.47$ e Å^{-5}, d[O5—CP] = 0.94 Å and d[H4—CP] = 0.23 Å. These results reveal, in light of Bader's (1990) atoms in molecules theory, the covalent character of the two O—H interactions of the short hydrogen bond. The Laplacians of the electron density, $\nabla^2\rho$ (CP), are negative and large in magnitude, and the electron densities, ρ (CP), are largely positive at the (3,−1) critical points of these interactions. These results are in agreement with neutron geometrical data, which show H4 nearer O5 than O4. However, considering the covalency, similar features were observed on the short symmetric hydrogen bonds of $(NH_3CH_3)(C_4H_5O_4)\cdot H_2O$ (Flensburg *et al.*, 1995) and $(NH_3CH_3)(C_4H_3O_4)$ (Madsen *et al.*, 1998). Of course, for a symmetric hydrogen bond the chemical environment is the same on both sides of the hydrogen bond.

It is helpful to compare the short O5—H4···O4 hydrogen bond with, for instance, the long N2—H21···O2 hydrogen bond, Figs. 5(*c*) and (*e*). The topological parameters at the (3,−1) CP of the H21···O2 interaction are $\rho = 0.18$ e Å^{-3}, $\lambda_1 = -1.16$ e Å^{-5}, $\lambda_2 = -1.14$ e Å^{-5}, $\lambda_3 = 3.34$ e Å^{-5}, $\nabla^2\rho = 1.04$ e Å^{-5}, d(O2—CP) = 1.27 Å and d(H21—CP) = 0.67 Å. These results agree with the curves plotted by Espinosa *et al.* (1999) for long hydrogen bonds and enable one to characterize this hydrogen bond as an electrostatic interaction. The Laplacian of the electron density, $\nabla^2\rho$ (CP), is positive and large in magnitude and the electron density, ρ(CP), is slightly positive at the (3,−1) critical points of these interactions.

This work has been supported by Minas Gerais Foundation for Research Development (FAPEMIG) under grant number CEX 1123/90. One of us (BLR) is grateful to FAPEMIG and the Brazilian Postgraduate Education Federal Agency (CAPES) for providing Graduate Fellowships.

References

Bader, R. F. W. (1990). *Atoms in Molecules.* International Series of Monographs on Chemistry 22. New York: Oxford University Press.
Becker, P. J. & Coppens, P. (1974). *Acta Cryst.* A**30**, 129–147.
Becker, P. J. & Coppens, P. (1975). *Acta Cryst.* A**31**, 417–425.
Blessing, R. H. (1988). *Acta Cryst.* B**44**, 334–340.
Burnet, M. N. & Johnson, C. K. (1996). *ORTEP*III. Report ORNL-6895. Oak Ridge National Laboratory, Tennessee, USA.
Coppens P. (1997). *X-ray Charge Densities and Chemical Bonding.* New York: Oxford University Press.
Cruickshank, D. W. J. (1961). *J. Chem. Soc.* pp. 5486–5504.
Dovesi, R., Causa, M., Orlando, R., Roetti, C. & Saunders, V. R. (1990). *J. Chem. Phys.* **92**, 7402–7411.
Espinosa, E., Souhassou, M., Lachekar, H. & Lecomte, C. (1999). *Acta Cryst.* B**55**, 563–572.
Fernandes, N. G., Tellgren, R. & Olovsson, I. (1990*a*). *Acta Cryst.* B**46**, 458–466.
Fernandes, N. G., Tellgren, R. & Olovsson, I. (1990*b*). *Acta Cryst.* B**46**, 466–474.
Flensburg, C., Larsen, S. & Stewart, R. F. (1995). *J. Phys. Chem.* **99**, 10686–10696.
Hansen, N. K. & Coppens, P. (1978). *Acta Cryst.* A**34**, 909–921.
Harel, M. & Hirshfeld, F. L. (1975). *Acta Cryst.* B**31**, 162–171.
Hirshfeld, F. L. (1971). *Acta Cryst.* B**27**, 769–781.
Hirshfeld, F. L. (1976). *Acta Cryst.* A**32**, 239–244.
Hirshfeld, F. L. (1977). *Isr. J. Chem.* **16**, 226–229.
Konstansek, E. C. & Busing, W. R. (1972). *Acta Cryst.* B**28**, 2454–2459.
Koritsanszky, T., Howard, S., Richter, T., Su, Z., Mallinson, P. R. & Hansen, N. K. (1995). *XD.* Freie University, Berlin.
Lundgren, J. O. (1982). *Crystallographic Computer Programs*, Report UUIC-B13-04–05. Institute of Chemistry, University of Uppsala, Sweden.
Madsen, D., Flensburg, C. & Larsen, S. (1998). *J. Phys. Chem. A*, **102**, 2177–2188.
Maslen, E. N., Fox, A. G. & O'Keefe, M. A. (1995). *International Tables for Crystallography*, edited by A. J. C. Wilson, Vol. C, pp. 476–512. Dordrecht: Kluwer Academic Publishers.
Moss, G. R., Souhassou, M., Blessing, R. H., Espinosa, E. & Lecomte, C. (1995). *Acta Cryst.* B**51**, 650–660.
Motz, D. & Albrand, K.-R. (1972). *Acta Cryst.* B**28**, 2459–2463.
Olovsson, I. & Jönsson, P.-G. (1976). *The Hydrogen Bond – Recent Developments in Theory and Experiment*, edited by P. Schuster, G. Zundel and C. Sandorfy, Vol. II, ch. 8. Amsterdam: North-Holland.
Savage, F. J., Blessing, R. H. & Wunderlich, H. (1987). *Trans. Am. Cryst. Assoc.* **23**, 97–100.
Sears, V. F. (1995). *International Tables for Crystallography*, edited by A. J. C. Wilson, Vol. C, pp. 383–391. Dordrecht: Kluwer Academic Publishers.
Siemens (1991). *XSCANS User's Manual*. Siemens Analytical X-ray Instruments Inc., Madison, Wisconsin, USA.
Souhassou, M., Espinosa, E., Lecomte, C. & Blessing, R. H. (1995). *Acta Cryst.* B**51**, 661–668.
Stevens, E. D., Lehmann, M. S. & Coppens, P. (1977). *J. Am. Chem. Soc.* **99**, 2829–2831.
Swaminathan, S., Craven, B. M. & McMullan, R. K. (1984). *Acta Cryst.* B**40**, 300–306.
Swaminathan, S., Craven, B. M., Spackman, M. A & Stewart, R. F. (1984). *Acta Cryst.* B**40**, 398–404.
Zavodnik, V., Stash, A., Tsirelson, V., De Vries, R. & Feil, D. (1999). *Acta Cryst.* B**55**, 45–54.